GLOBAL SUBSTORM EFFECT AND CONVECTION JET UNDER THE CONDITIONS OF CONTINUOUS EXTERNAL DRIVING: MULTI-SPACECRAFT OBSERVATIONS ON DECEMBER 22–23, 1996*)

Yu. I. Yermolaev, L. M. Zelenyi, N. L. Borodkova, R. A. Kovrazhkin, V. N. Lutsenko, A. A. Petrukovich, S. P. Savin, A. A. Skalsky

Space Research Institute, Russian Acad. Sci., Moscow, Russia

V. A. Sergeev

St. Petersburg University, St. Petersburg, Russia

T. Mukai

Institute of Space and Astronautical Science, Sagamihara, Japan

S.Kokubun

Solar-Terrestrial Environment Laboratory, Nagoya University, Japan

K. Liou, C.-I. Meng

Applied Physics Laboratory, Johns Hopkins University, Laurel, USA

G. Parks

Geophysics Program, University of Washington, Seattle, USA

J.-A. Sauvaud

Centre d'Etude Spatiale des Rayonnements, CNRS, University of Toulouse, France

Multipoint observations by ground-based stations and a fleet of ISTP satellites allowed us to study the plasma processes in different regions of the near-Earth space during a very interesting interval on December 22–23, 1996 which was characterized by ≈20 hour southward IMF B_z and almost constant solar wind pressure ≈ 1.2 nPa. Five substorm events were observed during this interval of continuous external driving. Several global effects of these substorms are described. In particular, comparison of measurements in the plasma sheet on both flanks showed (1) the similar loading/unloading processes in the tail correlated with substorm development, and (2) a strong bursty convection concentrated in a narrow ($\Delta Y \approx 15\,R_E$) channel. Observations show also that earthward bursty bulk flows (BBF) on both satellites likely coincide with appearance of auroral activity at the footpoints of corresponding satellites but there is no correlation between these flows observed on both flanks.

*) Presented at the NATO Advanced Research Workshop *Coordinated Studies of the Solar Wind-Magnetosphere-Ionosphere Interaction: Interball Observations*, held on September 7–11, 1998 in Kosice, Slovakia.

1 Introduction

One of the most important and challenging problem in the Solar-Terrestrial Physics program is the study of various manifestation of substorm dynamics and mechanisms of their generation. In direct or indirect way the solar wind is a driver of these processes and especially elucidating might be the study of this problem under special conditions of prolonged periods of southward interplanetary magnetic field (IMF). Southward IMF is favourable for reconnection of interplanetary and magnetospheric magnetic fields on the dayside magnetopause and should result in the enhancement of the magnetic flux in the tail, i.e., in the input of the solar wind energy into magnetospheric system [1, 2]. When the solar wind energy flux reaches a sufficient marginal level, substorms may be triggered directly by the changes in the solar wind and IMF [3] or by the IMF northward turnings [4]. On the other hand, under a sufficiently high level of the magnetic energy content in the tail the internal magnetospheric dynamics may result in substorm development [5]. Statistical studies of the substorms supports this point of view [6, 7]. Therefore, directly driven and loading/unloading processes are important for substorms [1].

The substorm is a large-scale phenomenon which essentially disturbs the plasma and magnetic field both in the magnetotail and in high latitude regions. It is important to make observations not only in these key regions (in the tail and the auroral regions) but also to study different channels of energy transport (steady convection, plasmoids, BBFs and so on) in the magnetosphere and to establish a cause-effect links between physical processes in the different parts of the system [1, 2, 8, 9].

The traditional picture of laminar earthward convection in the plasma sheet under the homogeneous large-scale dawn-dusk electric field has been questioned by the observations of plasma flows made at high temporal resolution. It appears (e.g. [10, 11]) that the main transport of mass, energy and magnetic flux in the midtail plasma sheet is realized via the short-lived high-speed plasma flows (bursty bulk flows, BBFs). The origin and spatial/temporal characteristics of transient features in the plasma sheet are not yet completely understood.

An unclear but important aspect is also the cross-tail scales of the convection pattern on different time scales. Simultaneous measurements with at least two spacecraft are required to resolve this issue. At the small ($\approx$1 min) time scale, the BBFs appeared to have a small size (less than $\approx 1/10$ of the tail diameter (e.g. [12, 9]). However, there were also some indications (in both event [13] and statistical studies, [14]) that the time-averaged ($\approx$1 h) convection features can also be very inhomogeneous in some events. Direct multi-spacecraft measurements of the average convection pattern, including its possible relationship to the BBF characteristics are highly desirable.

In this paper we present a unique case of $\approx$20 hour southward IMF and almost constant solar wind ram pressure. Simultaneous measurements of solar wind conditions on WIND, of mid-tail plasma sheet on INTERBALL/Tail Probe and GEOTAIL, and of auroral region on INTERBALL/Auroral Probe and POLAR are used for this analysis.

This type of continuous external forcing is rarely observed and few aspects of

it are quite interesting: the occurrence of substorm sequence and modification of convection in the plasma sheet due to the occurrence of substorms. A one more lucky coincidence in this interval is that the two spacecraft provided the measurements at comparable distances (25–30 R_E) downstream but in dawn and dusk parts of the plasma sheet at ≈20 R_E distance between them. This allows us to study a large scale behaviour and cross-tail structure of convection.

2 Observations

2.1 Survey of observations

For monitoring of interplanetary conditions we use the measurements of the WIND spacecraft located at $X \approx 80\,R_E$ and $Y < 20\,R_E$ during interval under investigation. To compare the WIND data with observations in the plasma sheet at the distance of $X = -30\,R_E$ we take into account of time of plasma and IMF propagation between satellites with the solar wind velocity V. After such time shifting the southward IMF commenced at ≈12 UT on December 22, 1996 and remained southward until ≈08 UT on December 23. As a result (Figure 1), the solar wind-induced cross-tail potential drop computed as

$$\Phi[kV] = 16(V/400)^2 + B\sin^3(\theta/2)$$

according to Boyle *et al.* [15] stayed at a high level throughout this time interval (with a few drops at 13–14, 17–20 and near 24 UT) and gradually declined after 04 UT on December 23 (IMF B_z was negative all that time). The nearly constant and low (≈1.2 nPa) ram pressure of the solar wind facilitates to view the variations of the lobe magnetic field (and tail pressure) as being related to the external driving and/or to the internal substorm effects.

Continuous strong external driving caused both the gradual development of the ring current (with maximal D_{st} depression ≈-40 nT reached ≈17 hours after the commencement of the southward IMF) and considerable electrojet activity in the auroral zone (Figure 1). Five substorm events could be recognized throughout this disturbed period as enhancements of the westward electrojet in Figure 1. The substorm onsets (see Table 1) occurred at 1251, ≈1625 and 2200 UT on December 22 (events 1–3), as well as at ≈0220, and ≈0815 UT on December 23 (events 4,5). These determinations were based on a large set of observations, including the UVI images of POLAR spacecraft (available for events 1,2,4), ground Pi2 pulsations (events 1,2,3,..) and both mid-latitude and auroral zone magnetograms (some subtle differences between different determinations are not important for present study but will be published separately). 1st and 5th substorm onsets were probably triggered by sharp positive variations of IMF B_z (seen as sharp drops of computed potential drop Φ in Figure 1), whereas no large triggers could be noticed for events 2,3,4 (referred later as the spontaneous onsets).

The plasma sheet parameters have been monitored by two spacecraft, INTERBALL/Tail Probe and GEOTAIL. Their GSM coordinates and MLT at substorm onsets are presented in Table 1. Most of the time both spacecraft stayed near the

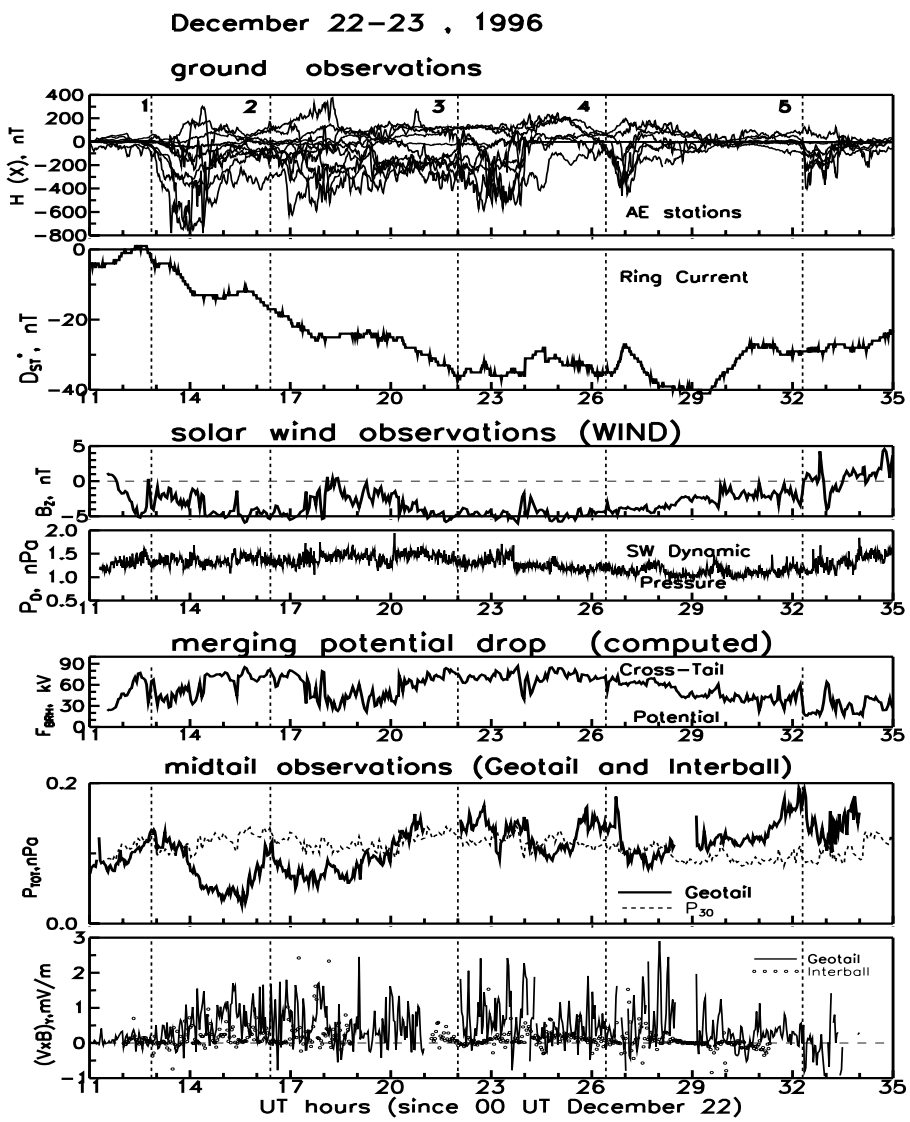

Fig. 1. Survey of solar wind, ground, and plasma sheet activity on December 22–23, 1996. From top to the bottom: a) superimposed magnetograms of 11 ground stations used to derive the standard AE index and SYM-H index of low-latitude magnetic variations which is a proxy for $D_{\rm st}$ index (denoted as $D_{\rm st}{}^{*}$); b) IMF B_z and solar wind ram pressure measured on WIND (shifted in time to $X = -30\,R_{\rm E}$ taking into account the solar wind speed); c) time variations of the expected cross-tail potential difference computed according to [15]; d) variations of the total (plasma plus magnetic) pressure and of the magnetic flux transport rate $(\mathbf{V} \times \mathbf{B})_y$ in the midtail according to Geotail measurements; the tail lobe magnetic pressure at $X = -30\,R_{\rm E}$ (P_{30}) computed for given solar wind conditions (according to [21]) is shown as a reference. Substorm onsets are shown by the dashed vertical lines.

Table 1. Substorm onsets, interplanetary conditions, and Geotail (GT) and Interball/Tail Probe (IT) locations

No	Onset Time UT	IMF B_z Change UT	INTERBALL/GEOTAIL Location					Comments
			SC	X_{GSM} R_E	Y_{GSM} R_E	Z_{GSM} R_E	MLT h	
	Dec.22							
1	1251	1215	IT	–23.4	12.2	–2.4	22.1	Triggered
			GT	–28.5	–10.8	–1.5	01.2	
2	1625	No	IT	–22.4	11.8	–2.0	22.1	Spontaneous
			GT	–27.9	–12.1	–3.0	01.3	
3	2200	No	IT	–20.2	10.9	–2.0	22.1	Spontaneous
			GT	–26.3	–13.8	–6.0	01.6	
	Dec.23							
4	0220	No	IT	–17.7	9.4	–4.4	22.2	Spontaneous
			GT	–24.6	–15.9	–5.0	02.2	
5	0815	0745	IT	–13.0	4.7	–8.3	22.2	Triggered
			GT	–22.0	–18.7	0.2	02.6	

neutral sheet at distances of 15–30 R_E from the Earth but GEOTAIL was in the dawn plasma sheet (during fifth event it exited to the magnetosheath) and INTERBALL was in the dusk plasma sheet.

During the most interesting time period between substorms 1 and 3, INTERBALL and GEOTAIL were at comparable distances from the Earth ($\approx$22 and $\approx$27 R_E) but a half way between the tail axis and the dusk and dawn flanks, respectively.

We used GEOTAIL magnetic field (MFI [16]) and plasma (LEP [17]) measurements at 12 s resolution. On INTERBALL/Tail Probe we used the magnetic field observations [18] and plasma observations made with two instruments. The moments of the distribution function from CORALL ion instrument covering the 0.05–25 keV energy range [19] were available at the spacecraft spin (2 min) resolution; we use only the V_x component of the flow (along the spacecraft spin axes) which, on the one hand, represents the most important component of the magnetospheric convection and, on the other hand, is less affected by the time variations of parameters during the 2 min spin period. The ELECTRON instrument provided the density and temperature of the plasma sheet electrons [20].

Variations of total (plasma plus magnetic) pressure in the tail (Fig. 1, bottom panel) show a systematic substorm response. In each substorm event, with either triggered or spontaneous onset, there was an increase of total pressure (loading) preceeding the onset. More than a half the time between the substorm onsets (ranging from 3.6 to 6.1 hours) there were no rapid changes of total pressure. At these times

the plasma convection was quite strong and variable, dominated by the bursty bulk flows (see the bottom panel of Figure 1). The most intense flows are seen during the 2–3 hour periods following the substorm onsets.

2.2 Plasma sheet during intense bursty plasma flows

Observed variability of the plasma flows can be due to both temporal variations and spatial effects when spacecraft crosses different parts of the flapping plasma sheet or even exits to the lobes. A favourable situation for probing the inner part of the plasma sheet (IPS, defined by the restriction that plasma β parameter was >0.5) occurred after 1330 UT (after the plasma sheet expansion associated with the first substorm) when INTERBALL stayed in the IPS for more that 8 hours, as indicated by low values of the B_x magnetic component in Figure 2 (left). GEOTAIL also spent a considerable time near the neutral sheet, but crossed it many times, so the B_x behaviour was much more variable. Therefore, to avoid the spatial effects we plotted in Figure 2 (right) only those 2 min averaged parameter values measured on GEOTAIL when it was in the IPS.

It should be noted that due to design features, the CORALL ion spectrometer on INTERBALL can underestimate the ion density. Consequently, we used plasma density from ELECTRON instrument together with ion temperature from CORALL to compute the total pressure on INTERBALL.

The plasmas measured by GEOTAIL and INTERBALL show some similarities as well as some differences. First of all, attention is drawn to the fact that a such large-scale phenomena as plasmoids and TCRs (they are shown by arrows on the second and third panels in Figure 3) are observed only on one from two satellites: plasmoids in the beginning of 1st and 4th substorms on Tail Probe and TCR in the beginning of 3rd substorm on GEOTAIL. This discrepancy allows us to estimate the sizes of these phenomena and location of magnetic field reconnection point in the tail during the substorm events. Third (right and left) panels in Figure 2 and second and third panels in Figure 3 present V_x component of ion velocity obtained on the INTERBALL/Tail Probe and GEOTAIL, respectively. V_x bursts are basically earthward and last about several minutes but there is no correlation between V_x velocity components observed on both satellites.

The plasma density value after the first substorm was about 0.1 cm^{-3} on both spacecraft. The temperatures were somewhat low for the disturbed conditions, on GEOTAIL the proton temperature changed from $\approx$2 keV to $\approx$4 keV during the time interval studied where the strongest flows were observed. On INTERBALL the proton temperature was somewhat higher, changing between $\approx$3 and $\approx$8 keV. This difference could be prescribed either to the azimuthal gradient (due to the ion acceleration in the electric field from dawn to dusk) or to the radial gradient (due to the smaller radial distance of INTERBALL than GEOTAIL). The electron temperature on INTERBALL changed in parallel to the proton temperature favouring the latter explanation. A clear temperature increase at $\approx$17 UT correlates with the B_z increase indicating once more the importance of heating in the compressed magnetic flux tube. Although similar sporadic earthward flows were observed between

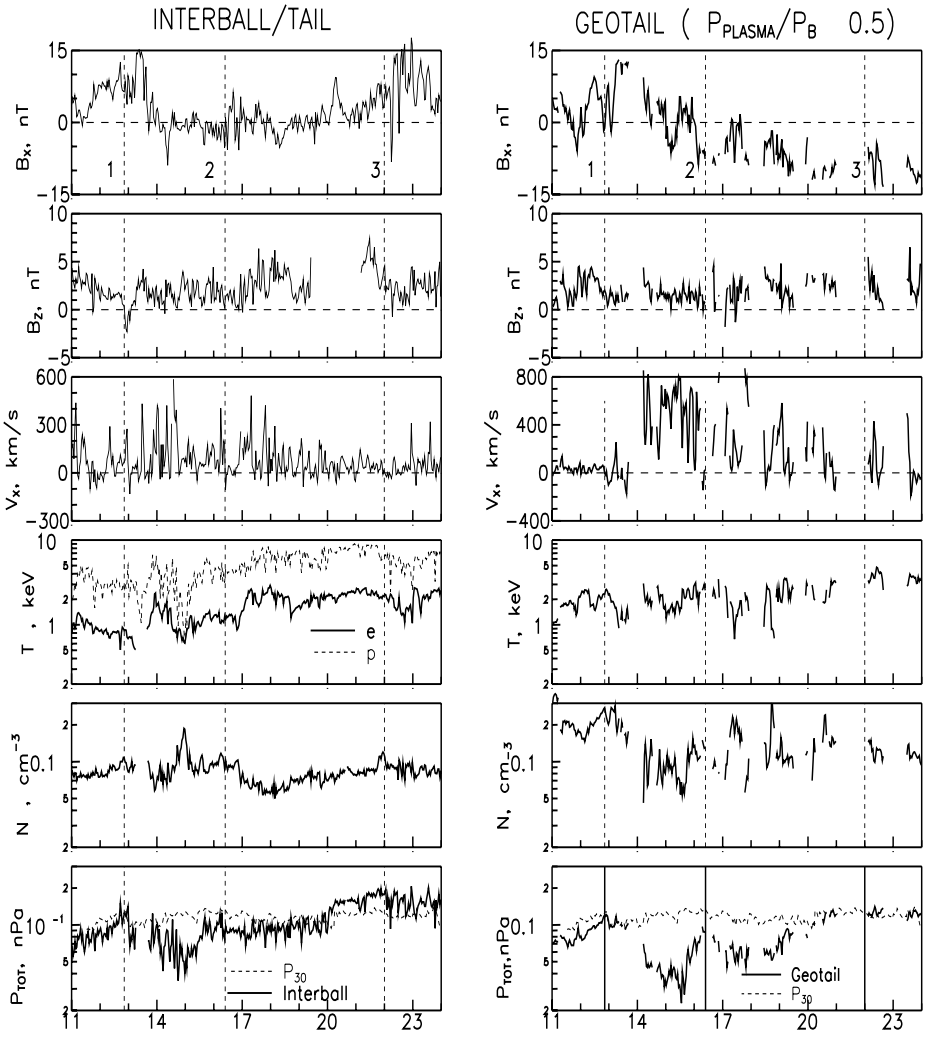

Fig. 2. Survey of plasma sheet parameters measured in the dusk plasma sheet (INTERBALL, left panels) and in the dawn plasma sheet (GEOTAIL, right panels). The tail lobe magnetic pressure P_{30} is shown for reference on the bottom panels. The onsets of substorms No. 1–3 are shown for reference. Note that only data in the inner plasma sheet are included for GEOTAIL.

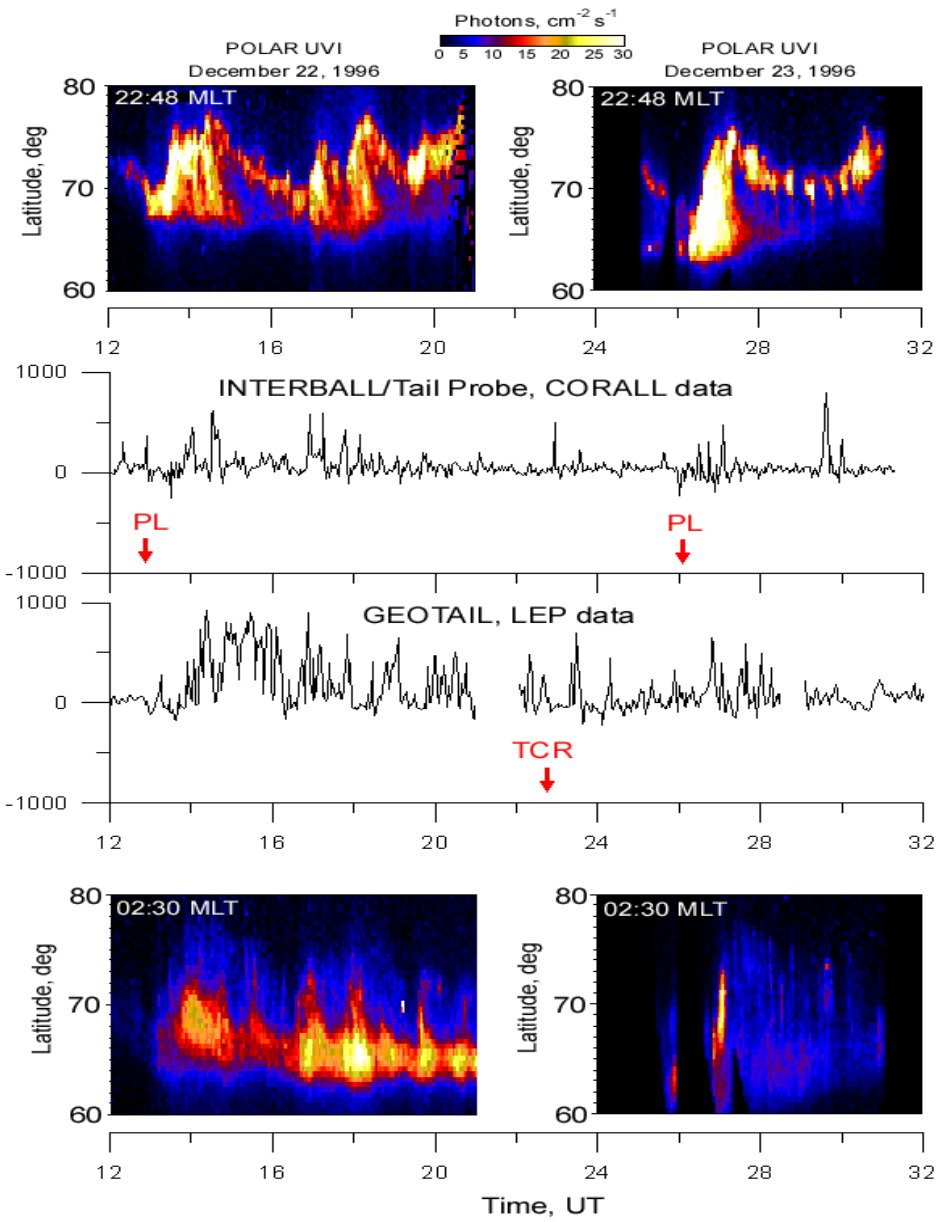

Fig. 3. Comparison of 30 min average values of the Earthward magnetic flux transport ($V_x \cdot B_z$) in the inner plasma sheet (under $P_{PL}/P_B > 0.5$) as measured on INTERBALL and GEOTAIL spacecraft. For reference we also show the amplitude of the expected cross-tail electric field (taken to be homogeneous) with the cross-tail potential 80 kV and tail diameter 50 R_E. The time variations of the cross-tail potential drop computed from solar wind parameters according to [15] are shown on the upper panel.

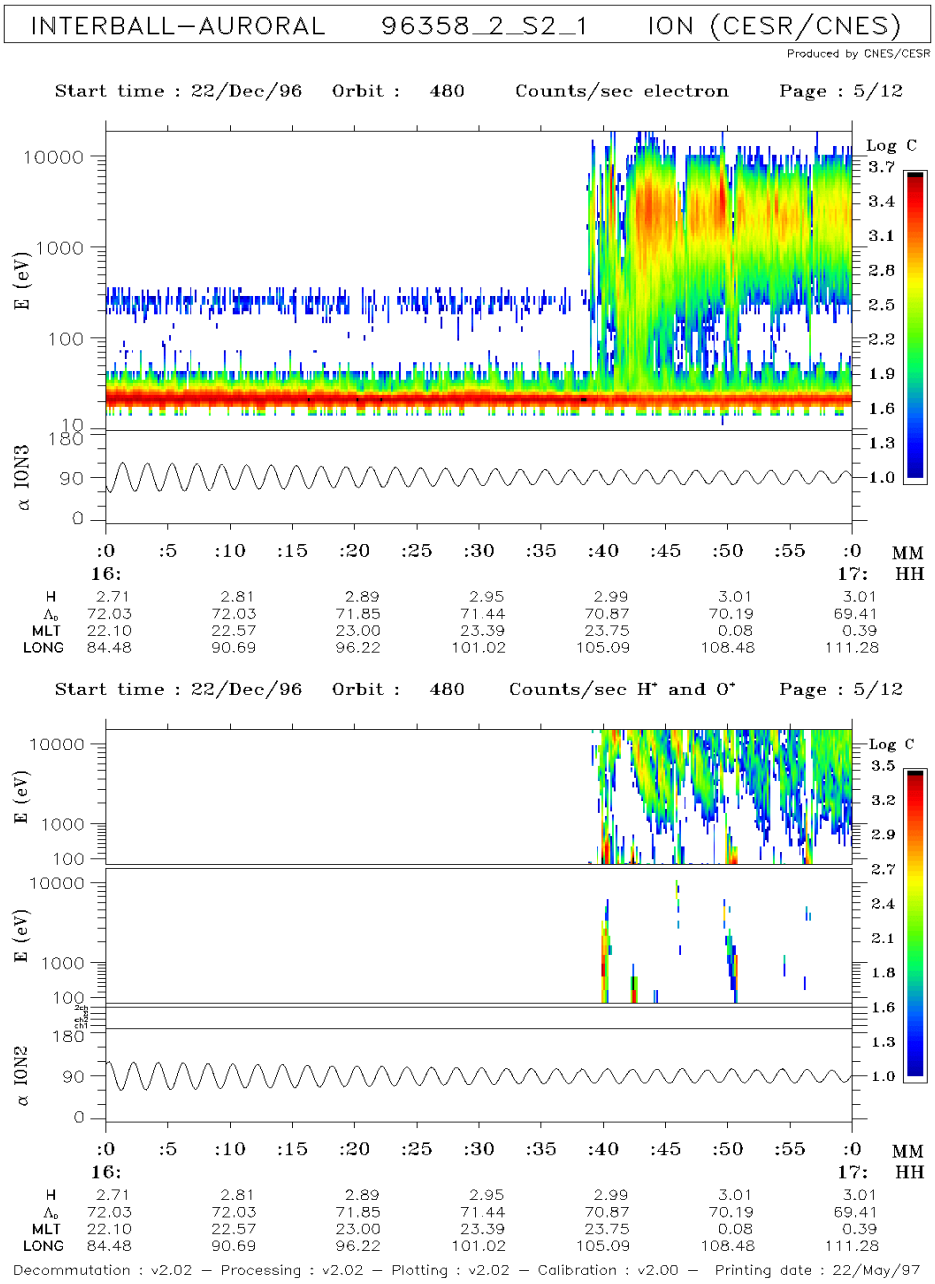

Fig. 4. Energy-time spectrograms for ions, O^+ and electrons during the INTERBALL/Auroral Probe pass through polar regions on 22 December, 1996.

1330 and 1500 UT on INTERBALL, they did not produce comparable acceleration. The B_z values in that case did not change much and stayed small, about 2 nT. The fast flows in the IPS region were exclusively in the earthward direction on both spacecraft, this is also true for high speed observed during the loading and unloading phases (see GEOTAIL data for substorm 2), as well as during the episodes of steady total pressure.

A remarkable feature of the time interval considered here is the low total pressure between 14 and 19 UT, which is smaller than the average lobe magnetic field pressure (P_{30}) computed according to Fairfield and Jones [21] and shown as the reference level in the bottom plots in Figure 2. During this time interval the strongest flows were observed at both spacecraft, but with higher speed flows on the GEOTAIL. These features are of great interest and they will be discussed in the section 3.2.

2.3 Auroral observations

The top and bottom color panels in Figure 3 are keograms made from POLAR UVI images at LBHL band [22] showing the auroral dynamics in the AACGM ("Latitude - UT") coordinates [23] at two meridians, 22.40 MLT (top) and 02.30 MLT (bottom), i.e., at the footpoints of Tail Probe and GEOTAIL, respectively. Note that the LBHL auroral emission is approximately proportional to the total energy input of precipitating electrons [24, 25] and, therefore, can be used as a proxy of the hemispheric energy input. Both panels show strong auroral activity during the interval studied. Nevertheless, there are significant differences between the two pictures. Increases in brightness and poleward expansions of the aurora in the top panel coincide with substorm activity and have characteristic recurrence period about 3–6 hours. The bottom panel does not show this dependence: increases in brightness occur with periodicity about 1 hour and there is no poleward expansions of the aurora. Data presented in Figure 3 allows to suggest that observations of BBFs on each satellite coincide with appearances of auroral activity in footpoint of corresponding satellite.

During the interval studied POLAR and INTERBALL/Auroral Probe had several orbits such a way that there were auroral zone and polar cap observations during substorms. Detailed analysis of these data will be the subject of further investigations. Here we only present an example of data and note several large-scale phenomena observed by satellites.

Figure 4 presents ion, O^+ and electron energy spectrograms measured with ION instrument on INTERBALL/Tail Probe [26] during the time interval of 1600–1700 UT on December 22. In auroral zone, which began at ≈1638 UT, the ION instrument observed ion injections with periodicity about 1–2 min and time-of-flight energy dispersion. Simultaneously with the injections the upward O^+ fluxes with energy up 10 keV were observed. Estimates made on the basis of this dispersion show that these ion fluxes probably originated at the distance $\approx$ 15–20 R_E from the observation point, i.e., not far (but nearer to the Earth) from Tail Probe and GEOTAIL locations. At the same time ≈1640 UT, large deviation of magnetic field

measured on Auroral Probe from the model field were observed, i.e., there were currents which disturbed the magnetic field in this region. This time coincides with the poleward aurora expansion observed with POLAR UVI instrument.

3 Discussion

3.1 Substorms during conditions of continuous driving

There have not been many studies of substorms during conditions of continuous driving, especially concerning the characteristics of loading/unloading processes. Our study shows that the duration of both loading and unloading episodes (0.5–1 hour) is similar to those for the classic substorms. In events 2,4,5 the loading episodes do not correlate with any change of the solar wind parameters which shows that the occurrence of the loading phase during steady energy supply from the solar wind is controlled by the internal dynamics of the magnetotail. It is also of interest that four similar sharp positive IMF B_z excursions (sharp decreases of potential drop in the middle panel of Figure 1) have been observed at ≈1240, ≈1715, ≈2340 UT on December 22 and ≈0800 UT on December 23. However only first and last of them, which were preceded by the loading episodes, could trigger the 1st and 5th substorms. This is a good illustration to show that the magnetotail should be prepared for the expansion phase to be triggered by the IMF discontinuity.

The time intervals between the onsets of five successive substorms were 3.5, 5.7, 3.7, and 6.1 hours, respectively. Their length seems to be inversely related to the average values of the expected potential drop between substorms (61, 55, 81, and 52 kV, see Figure l). These values of inter-substorm time length are larger than the average substorm recurrence time 2.7 hours reported by Borovsky *et al.* [7] and much larger than ≈50 min recurrence time found by Farrugia *et al.* [27] for similar conditions of strong steady energy supply. In our case the substorms were truly global reconfiguration events determined from both loading/unloading features in the tail. It will be important to revisit this issue with the more extended data set. A new observation is that during a considerable part (more than a half) of the time interval between substorms the total pressure is nearly constant and plasma sheet convection is quite strong. These episodes resemble the long-duration periods of steady magnetospheric convection (SMC, e.g. [13]) but in our case these episodes last 2–3 hours and intervene between the expansion and growth phases of successive substorms.

POLAR UVI measurements showed that substorms were accompanied by poleward expansions of auroral brightness at ≈2230 MLT (Tail Probe footpoint) and such auroral motions were not observed at ≈0230 MLT (GEOTAIL footpoint). BBFs observed in the plasma sheet during substorms and between them are likely correlated with auroral intensifications in the footpoint of corresponding satellite. During substorms Auroral Probe observed ion injections with energy dispersion correlated with upward O^+ ion fluxes with energy up 10 keV and disturbances of magnetic field which are probably connected with local electric currents. Estimates made for 2nd substorm at ≈1630 UT on December 22 showed that these injec-

tions were generated at distances of ≈15–20 R_E, that is, nearer to the Earth than GEOTAIL and INTERBALL/Tail Probe, but not far from them. The example of ion injections presented here (see Figure 4) is interesting because only during this substorm the plasmoids (or TCR as for 3rd substorm) were not observed on Tail Probe and GEOTAIL. So, it is possible to suggest that only during this substorm the point of reconnection of tail magnetic field was located farther from the Earth than Tail Probe and GEOTAIL locations, (–22,12,–1) and (–24,–13,–3) R_E in GSM frame, respectively. In other cases the reconnection region are likely to be nearer Earth than the Tail Probe and GEOTAIL locations, i.e., nearer than –22 R_E, and the region of generation of ion injections may coincide with region of field reconnection. This estimate is in agreement with our recent result (15–16 R_E) obtained on the basis of INTERBALL/Tail Probe and GEOTAIL observations [28].

3.2 Convection jet feature in the plasma sheet

Figure 5 presents the half-hour averages of the $V_x \cdot B_z$ values in the inner part of the plasma sheet (the averages were plotted only if the measurements in the IPS occupied at least 10 minutes of entire 30 min averaging time interval). These values give a good proxy of the earthward magnetic flux transport $(\mathbf{V} \times \mathbf{B})_\mathbf{y}$ as was checked using GEOTAIL data. In steady state configuration the total average earthward flux transport (E_y integrated across the tail) should correspond to the cross-tail potential drop Φ, and for $\Phi = 80$ kV (computed according to Boyle *et al.* [15] top panel in Figure 5) and tail radius 25 R_E (computed using the Shue *et al.* [29] formula) the expected average flux transport rate should be $E_0 \approx 0.25$ mV/m. The INTERBALL-based estimate gives an average $V_x \cdot B_z$ value about the E_0 value. On GEOTAIL, during three hours (14 to 17 UT) the flux transport rate was ≈3 times larger than on INTERBALL. Note (Figure 2) that most of this time the tail pressure was nearly steady and it was considerably reduced as compared to its average value. The observation of stronger convection in the dawn plasma sheet is not inconsistent with the auroral zone magnetometer data. Between 13 and 17 UT the deepest negative magnetic bay which forms a lower envelope in the magnetogram plot in Figure 1 (top) came from Barrow station (≈69° of CGLat, magnetic midnight at ≈12.5 UT). This confirms that the strongest auroral electrojet currents occurred in the high-latitude portion of the postmidnight auroral oval.

The observation of long-duration enhanced convection regions is not unique. Nishida *et al.* [14] compared daily averages of $\mathbf{V} \times \mathbf{B}$ measured by GEOTAIL at ≈95 R_E during long active period and found a distinct peak of the magnetic flux transport rate (0.43 mV/m) in premidnight sector. In the event studies reported by Sergeev and Lennartsson [13], and Nakamura *et al.* [30] the average transport rates were about 3–4 times higher when compared to E_0 in the premidnight sector of plasma sheet. In both cases the observations were performed during an interval of several hours following the substorm when the reduced total pressure was also observed. For the first time our results provide direct evidence of strong long-term inhomogeneity in the plasma sheet convection, but here the convection jet occupied the dawn half of plasma sheet. The location of the convection jet, thus, may vary

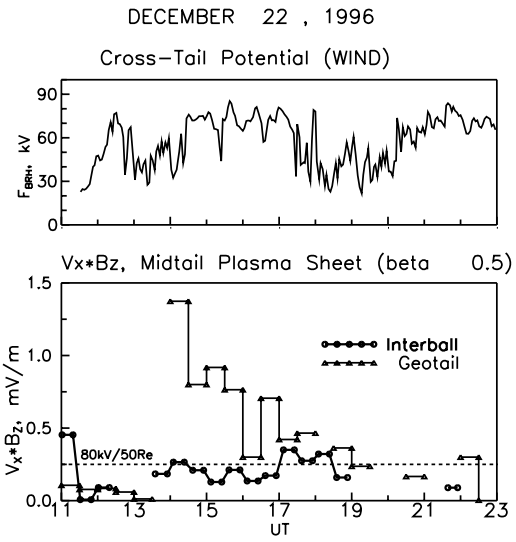

Fig. 5. BBF observations on dusk (INTERBALL/Tail Probe, 3rd plate) and dawn (GEOTAIL, 2nd plate) flanks of plasma sheet and POLAR UVI keogram in corresponding footpoints (1st and 4th plates).

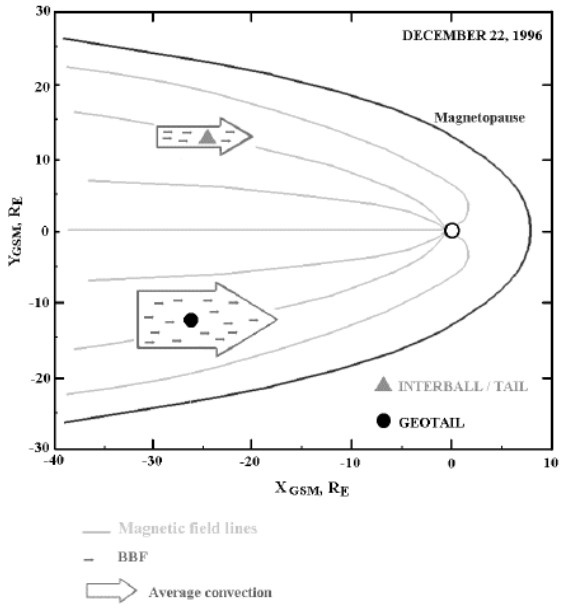

Fig. 6. Schematic view of the convection jet pattern.

from one event to another and even change during an event.

The upper estimate of the possible cross-tail width of the convection jet in the plasma sheet ΔY is about $15\,R_{\rm E}$ (1/3 of tail diameter $D_{\rm T}$ with $E_{\rm y}^{\rm GT} \simeq 3E_0$ in the convection jet region to get the right cross-tail potential drop value, that is, $\Delta Y \simeq (E_0/E_{\rm y}^{\rm GT}) \cdot D_{\rm T} \simeq 1/3 \cdot 50\,R_{\rm E}$) [31]. The large-scale pattern of the convection jet in geomagnetic equator is illustrated by Figure 6 where the triangle and circle show satellite positions, small arrows — BBFs, and large arrows — average large-scale convection at the position of the corresponding satellite.

It is of note that the differences between the 0.5 hour average $V_x \cdot B_z$ values on GEOTAIL and INTERBALL decreased with time and after 17 UT (following the 2nd substorm), both values became comparable to the expected cross-tail electric field E_0. Whether it reflects any inherent dynamics of the convection jet or was caused by the spatial variation (exit of GEOTAIL from convection stream) cannot be stated for sure.

This long-term inhomogeneity of convection could be an important factor which influences the 3D current system and magnetic configuration of the tail (e.g. [12]). The origin of the convection jet phenomenon should be related to the high intensity/occurrence rate of the bursty bulk flows at distances $r > 30\,R_{\rm E}$ which, being averaged, forms the observed enhanced convection. One possibility concerns the inhomogeneous reconnection rate in the far tail which depends on the Alfvén speed in the lobe adjacent to the plasma sheet and, therefore, on the distribution of the cold plasma density (e.g. [13]). More observations are required to understand the physics of these phenomena.

4 Conclusions

We presented several preliminary results of multi-point observations during a $\approx$ 20 hour interval of southward IMF and low steady solar wind pressure on December 22–23, 1996. Five substorm events with distinct loading/unloading features in the midtail were observed during the continuous external forcing. The loading features did not necessarily correlate with the changes of solar wind parameters which implies that switching to the loading can be determined by the internal magnetotail dynamics. The substorm recurrence time, 3.6 to 6.1 hours, appeared to be larger than the values previously reported by Borovsky *et al.* [7] and Farrugia *et al.* [27] and inversely depended on the average rate of magnetic flux supplied to the magnetotail. During about half the time interval between substorms the configuration was locally steady with no considerable change of total pressure but with intense convection in the plasma sheet resembling the steady convection episodes.

A unique possibility of simultaneous observations of convection in the inner plasma sheet by GEOTAIL and INTERBALL/Tail Probe during more than 8 hours gave direct evidence that on the long term the magnetic flux transport rate may be very inhomogeneous in the tail for many hours. The short ($\approx$ 1 min) earthward bursty bulk flows (BBF) on both satellites likely coincide with appearance of auroral activity at the footpoints of corresponding satellite but there is no correlation between these flows observed on both flanks. The large-scale phenomenon of con-

vection jet appears to be due to the grouping of the most intense bursty bulk flows in the localized portion of the plasma sheet. The location of convection jet in the dawn plasma sheet presented here differed from that in previous observations of enhanced convection [13, 14, 30] which placed the convection jet in the premidnight plasma sheet. More observations are necessary to establish the morphology and origin of the convection jet phenomenon.

We are grateful to INTERBALL/Tail and Auroral Probe magnetic field group for providing data. We thank R. P. Lepping and K. W. Ogilvie (the WIND spacecraft) for making available to us the data of their experiments. We also thank T. Iyemori (WDC-C1, Kyoto) for the high-resolution data of SYM index. The work at IKI was supported by the INTAS Grant No. 96-2346. The work by VAS was financially supported by the RFBR grant No. 98-05-04114. The Editor thanks Tuija Pulkkinen for her assistance in evaluating this paper.

References

[1] D.N. Baker: in *Substorms 1*, ESA-SP 335, 1992, p.185.

[2] V.A. Sergeev, R.J. Pellinen, and T.I. Pulkkinen: Space Sci. Rev. **75** (1996) 551.

[3] S.-I. Akasofu: Space Sci. Rev. **28** (1981) 121.

[4] G. Rostoker: in *High-Latitude Space Plasma Physics*, (B. Hultqvist, T. Hagfors) Plenum Publ. Co., New York, 1983, p.189.

[5] D.N. Baker, A.J. Klimas, R.L. McPherron, and J. Büchner: Geophys. Res. Lett. **17** (1985) 41.

[6] Y. Kamide, P.D. Perrault, S.-I. Akasofu, and J.D. Winningham: J. Geophys. Res. **82** (1988) 5521.

[7] J.E. Borovsky, R.J. Nemzek, and R.D. Belian: J. Geophys. Res. **98** (1993) 3807.

[8] V. Angelopoulos, W. Baumjohann, C.F. Kennel, F.V. Coroniti, M.G. Kivelson, R. Pellat, R.J. Walker, H. Luhr, and G. Paschmann: J. Geophys. Res. **97** (1992) 4027.

[9] V. Angelopoulos *et al.*: Geophys. Res. Lett. **24** (1997) 2271.

[10] W. Baumjohann: Space Sci. Rev. **64** (1993) 141.

[11] V. Angelopoulos *et al.*: J. Geophys. Res. **101** (1996) 4967.

[12] V.A. Sergeev, V. Angelopoulos, J.T. Gosling, C.A. Cattell, and C.T. Russell: J. Geophys. Res. **101** (1996) 10817.

[13] V.A. Sergeev and W. Lennartsson: Planet. Space Sci. **36** (1988) 353.

[14] A. Nishida, T. Mukai, T. Yamamoto, Y. Saito, and S. Kokubun: Geophys. Res. Lett. **22** (1995) 2453.

[15] C.B. Boyle, P.H. Reiff, and M.R. Hairstone: J. Geophys. Res. **102** (1997) 11.

[16] S. Kokubun, T. Yamamoto, M.H. Acuna, K. Hayashi, K. Shiokawa, and H. Kawano: J. Geomag. Geoelectr. **46** (1994) 7.

[17] T. Mukai, S. Machita, Y. Saito, M. Hirahara, T. Terasawa, N. Kaya, T. Obara, M. Ejiri, and A. Nishida: J. Geomag. Geoelectr. **46** (1994) 669.

[18] S. Klimov *et al.*: Ann. Geophys. **15** (1997) 514.

[19] Yu.I. Yermolaev, A.O. Fedorov, O.L. Vaisberg, V.M. Balebanov, Yu.A. Obod, R. Jimenez, J. Fleites, L. Llera, and A.N. Omelchenko: Ann. Geophys. **15** (1997) 533.

[20] J.-A. Sauvaud, P. Koperski, T. Beutier, H. Barthe, C. Aoustin, J.J. Thocaven, J. Rouzaud, E. Penou, O. Vaisberg, and N. Borodkova: Ann. Geophys. **15** (1997) 587.

[21] D.H. Fairfield and J. Jones: J. Geophys. Res. **101** (1996) 7785.

[22] M.R. Torr *et al.*: Space Sci. Rev. **71** (1995) 329.

[23] K.B. Baker and S. Wing: J. Geophys. Res. **94** (1989) 9139.

[24] D.J. Strickland, R.E. Daniel, Jr., J.R. Jasperse, and B. Basu: J. Geophys. Res. **98** (1993) 21533.

[25] G.A. Germany, M.R. Torr, D.G. Torr, and P.G. Richards: J. Geophys. Res. **99** (1994) 383.

[26] J.-A. Sauvaud, H. Barthe, C. Aoustin, J.J. Thocaven, J. Rouzaud, E. Penou, D. Popescu, R.A. Kovrazhkin, and K.G. Afanasiev: Ann. Geophys. **16** (1998) 1056.

[27] C.J. Farrugia, M.P. Freeman, L.F. Burlaga, R.P. Lepping, and K. Takahashi: J. Geophys. Res. **98** (1993) 7657.

[28] A.A. Petrukovich *et al.*: J. Geophys. Res. **103** (1998) 47.

[29] J.-J. Shue, J.K. Chao, H.C. Fu, C.T. Russell, P. Song, K.K. Khurana, and H.J. Singer: J. Geophys. Res. **102** (1997) 9497.

[30] R. Nakamura, S. Kokubun, L. Bargatze, T. Mukai, T. Yamamoto, T. Nagai, K.B. Baker, M.R. Hairston, P.H. Reiff, and O.A. Troshichev: in *Proc. of* 4^{th} *Intern. Conf. on Substorms*, 1998 (in press).

[31] Yu.I. Yermolaev, V.A. Sergeev, L.M. Zelenyi, A.A. Petrukovich, J.-A. Sauvaud, T. Mukai, and S. Kokubun: Geophys. Res. Lett. **26** (1999) 177.